

Order, Disorder, and Transitions in Decorated AKLT States on Bethe Lattices

Nicholas Pomata^{1,*}

¹*C. N. Yang Institute for Theoretical Physics and Department of Physics and Astronomy,
State University of New York at Stony Brook, Stony Brook, NY 11794-3840, USA*

(Dated: today)

Returning to one of the original generalizations of the AKLT state, we extend prior analysis on the Bethe lattice (or Cayley tree) to a variant with a series of n spin-1 decorations placed on each edge. The recurrence relations derived for this system demonstrate that such systems are “critical” for coordination numbers $z = 3^{n+1} + 1$, demonstrating order for greater and disorder for lesser coordination number. We then generalize further, effectively interpolating between systems with different values of n , using two realizations, one isotropic under local $SU(2)$ transformations and one anisotropic. Exact analysis of these recurrence relations allows us to deduce the location and behavior of order-disorder phase transitions for $z > 4$.

I. INTRODUCTION

The valence-bond states developed by Affleck, Kennedy, Lieb, and Tasaki [1] (AKLT), foundational for the tensor-network formalism, provided a useful framework to explore strongly-interacting systems. The one-dimensional states originally explored are particularly amenable to study due to the transfer-matrix analysis they admit. However, much as with classical spin models that admit a similar analysis in one dimension, AKLT’s higher-dimensional generalizations [2] are largely quite difficult to ascertain exact information about, effectively because loops in higher-dimensional lattices obstruct such a transfer-matrix approach. There is one notable exception: the Bethe lattice, or Cayley tree, an infinitely-branching graph with an identical number of edges (the degree or coordination number z) per site, on which AKLT formulated exact recurrence relations that enabled them to determine exact properties of this system. Following their work, Fannes, Nachtergaele, and Werner established more thorough conclusions, analyzing the state using the quantum Markov chain formalism to rigorously investigate the possible states on the infinite lattice [3, 4].

The Bethe lattice, while generally unphysical due to its exponentially-growing vertices¹, has attracted attention for use as a test bed for tensor network systems, especially infinite tensor-

* nicholas.pomata@stonybrook.edu

¹ Because of this, the Bethe lattice cannot be embedded in Euclidean space with both strictly finite node density and bounded edge length. However, as shown in Fig. 1, it can be embedded in hyperbolic space in interesting, if not necessarily physically relevant, ways.

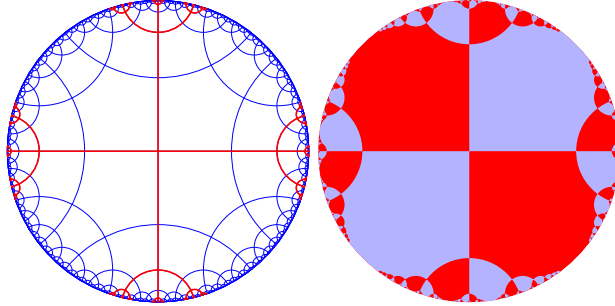


FIG. 1. The Bethe lattice can be embedded in hyperbolic geometry in regular ways: e.g. as (a) a sublattice of a more conventional tiling (here the degree-4 Bethe lattice within the order-4 pentagonal tiling) or as (b) the edge set of a tiling by infinite-sided shapes, or apierogons.

network systems with the development of the quantum Markov chain formalism to rigorously define infinite tensor-network states [5–7], and as a kind of mean-field theory variant. This includes analysis of Hamiltonians on the Bethe lattice without exact ground states, using variants of the density-matrix renormalization group [8] and the time-evolving block decimation algorithm [9] to extract approximate ground states and analyze their phase diagrams.

In this work, we will return to the AKLT state on the Bethe lattice, this time adding decorations on each edge as was done in [10, 11] to make two-dimensional AKLT systems more amenable to study. In Section II, we will extend the methods of [2] to these systems and obtain exact recurrence relations, including indications of critical behavior in some cases. In Section III, we will describe observables that can be used to validate the idea of such long-ranged behavior on an infinite disordered state. In Section IV, we will then describe continuous extensions of these decorated systems and show that these exhibit phase transitions with critical features that can be described exactly. Finally, in Section V, we will examine the somewhat complicated phase diagram that occurs from this when the system explicitly breaks $SU(2)$ symmetry.

II. BASIC RECURRENCE RELATIONS

In determining the behavior of the AKLT model on decorated lattices, we will, for the most part, follow the derivation given by AKLT [2] of the behavior of the model on the “bare” Bethe lattice. In particular, we will start by considering finite systems with antiferromagnetic boundary conditions; we will then extend that analysis to make tentative conclusions about the the systems as may be defined in infinite-size frameworks where the translation symmetry of the Bethe lattice is possible.

The derivation starts with the expression for the norm-squared of an AKLT state Ψ_A on a bipartite graph A (from the equation shortly before (4.8) of [2])

$$\langle \Psi_A | \Psi_A \rangle = \sum_{G, G'} \prod_{i \in A} \delta(m_i(G), m_i(G')) m_i(G)! (z_i - m_i(G))!. \quad (1)$$

Here

- G and G' are subgraphs (alternatively, edge subsets) of A ,
- z_i is the connectivity of vertex i in the graph A (which equals z on the sites of the bare lattice and 2 on the decorations),
- $m_i(G)$ is the connectivity of vertex i in the graph G , and
- δ is the Kronecker delta symbol.

For the sake of brevity, we will for the remainder of this section use the function

$$c_z(n) \equiv n!(z - n)! = \frac{z!}{\binom{z}{n}}.$$

We may interpret n_i as the physical index of spin i in the S_z basis *on every other site of A* ; that is, if we bipartition A with some $\text{sgn}(i)$ that maps alternating sites to $+1$ and -1 , we can identify the S_z index of *any* spin i with $z/2 + \text{sgn}(i)(m_i - z/2)$. In particular, we can insert a matrix M_{ab} contracted with the physical indices at site i by modifying

$$\begin{aligned} & \delta(n_i(G), m_i(G')) c_{z_i}(m_i(G)) \Rightarrow \\ & \sqrt{c_{z_i}(m_i(G)) c_{z_i}(m_i(G'))} \\ & \times \begin{cases} M_{m_i(G), m_i(G')} & \text{sgn}(i) = +1 \\ M_{z_i - m_i(G), z_i - m_i(G')} & \text{sgn}(i) = -1 \end{cases}. \end{aligned}$$

When considering a finite system, we will within this section use what we may call “classical” boundary conditions, in which boundary qubits are fixed to be either spin-up or spin-down. That is, when considering a system with radius M , we eliminate the physical spins at a distance $M + 1$ or more from the origin and replace the virtual singlets connecting sites of distance M and $M + 1$ from the origin with up or down spins. (This is the only sort of configuration considered in [2, , shortly before 4.8]). In that case, the only admissible configurations in (1) are ones in which G and G' coincide exactly, i.e. as in [2, , eq. 4.8], the equation reduces to

$$\langle \Psi_A | \Psi_A \rangle = \sum_{G \subset A} \prod_{i \in A} c_{z_i}(m_i(G)). \quad (2)$$

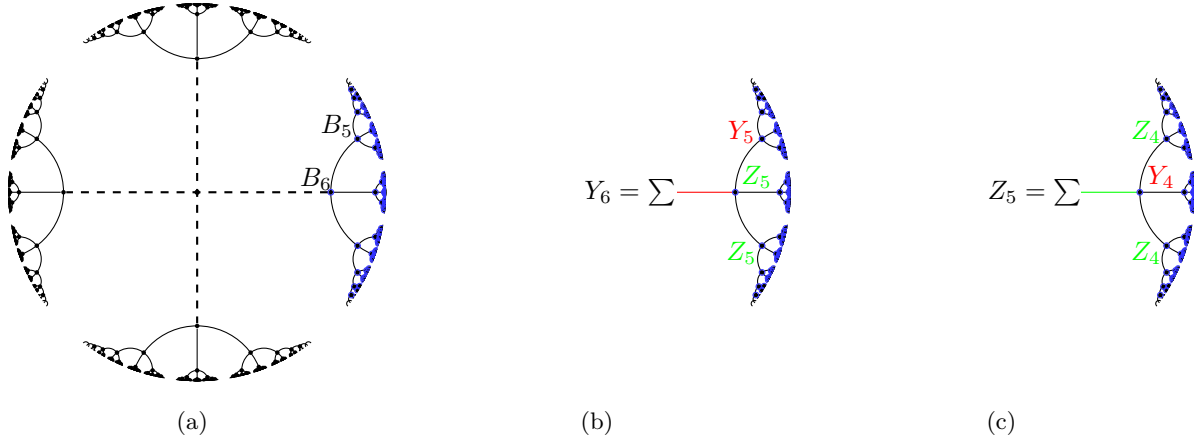


FIG. 2. Factoring the expression (2) for the norm of the AKLT state into “branches” of the Bethe lattice. (a) We label branches of a finite lattice (equivalent under “rotations”) by the distance of the root node from the boundary. (b) The values Y_M and Z_M , corresponding to inclusion in or exclusion from G , are determined from Y_{M-1} and Z_{M-1} given the possible configurations. (c) These in turn have been determined from Y_{M-2} and Z_{M-2} .

The recursive solution used relies on the ability to factor branches of the “Cayley tree” out of this expression, in what is a variant on a transfer-matrix approach. Again as in [2], and as shown in Fig. 2, we define Y_M and Z_M as the value of the factor corresponding to a depth- M branch B_M when the edge that connects that branch to the origin is, respectively, included in or excluded from G . That is (if we consider $i = 0$ to be the origin of the branch B_M),

$$Y_M \equiv \sum_{G \subset B_M} c_z(m_0(G) + 1) \prod_{k \in B_M} c_{z_k}(m_k(G)) \quad (3)$$

$$Z_M \equiv \sum_{G \subset B_M} c_z(m_0(G)) \prod_{k \in B_M} c_{z_k}(m_k(G)) \quad (4)$$

$$\|\Psi_M\|^2 = \sum_{m=0}^z \binom{z}{m} c_z(m) Y_M^m Z_M^{z-m} = z! \sum_{m=0}^z Y_M^m Z_M^{z-m}. \quad (5)$$

(We are, for now, only considering the bare lattice; while (3) and (4) remain correct for the decorated lattice, (5) will need to be modified.)

In analyzing the bare lattice in [2], AKLT factor the sub-branches of B_M out as well to yield

recurrence relations for Y_M and Z_M :²

$$\begin{aligned} Y_M &= \sum_{m=0}^{z-1} (z-1)!(m+1)Y_{M-1}^m Z_{M-1}^{z-m-1} \\ Z_M &= \sum_{m=0}^{z-1} (z-1)!(z-m)Y_{M-1}^m Z_{M-1}^{z-m-1} \end{aligned} \quad (6)$$

We can modify this approach to suit the n -fold decorated lattice by treating each decoration as the root of its own branch: that is, let $B_M^{(0)} = B_M$ be a branch with a degree- z vertex as its root (and a depth *in degree- z vertices* of M) and $B_M^{(k)}$ be that branch with k decorations. The primary modifications to (5) and (6) consist in changing z to 2 as appropriate:

$$\begin{aligned} Y_M^{(0)} &= (z-1)! \sum_{m=0}^{z-1} (m+1)(Y_{M-1}^{(n)})^m (Z_{M-1}^{(n)})^{z-m-1} \\ Y_M^{(k)} &= 2Y_M^{(k-1)} + Z_M^{(k-1)}, \quad k > 0 \\ Z_M^{(0)} &= (z-1)! \sum_{m=0}^{z-1} (z-m)(Y_{M-1}^{(n)})^m (Z_{M-1}^{(n)})^{z-m-1} \\ Z_M^{(k)} &= Y_M^{(k-1)} + 2Z_M^{(k-1)}, \quad k > 0 \end{aligned} \quad (7)$$

The $k > 0$ case is a simple linear relation that we can solve as a matrix equation:

$$\begin{aligned} \begin{pmatrix} Y_M^{(n)} \\ Z_M^{(n)} \end{pmatrix} &= \begin{pmatrix} 2 & 1 \\ 1 & 2 \end{pmatrix} \begin{pmatrix} Y_M^{(n-1)} \\ Z_M^{(n-1)} \end{pmatrix} = \begin{pmatrix} 2 & 1 \\ 1 & 2 \end{pmatrix}^n \begin{pmatrix} Y_M^{(0)} \\ Z_M^{(0)} \end{pmatrix} \\ &= \begin{pmatrix} \frac{3^n+1}{2} & \frac{3^n-1}{2} \\ \frac{3^n-1}{2} & \frac{3^n+1}{2} \end{pmatrix} \begin{pmatrix} Y_M^{(0)} \\ Z_M^{(0)} \end{pmatrix}. \end{aligned} \quad (8)$$

Combining (7) with (8), we get

$$\begin{aligned} Y_{M+1}^{(n)} &= \frac{(z-1)!}{2} \sum_{i=0}^{z-1} [(3^n+1)(i+1) + (3^n-1)(z-i)] (Y_{M-1}^{(n)})^m (Z_{M-1}^{(n)})^{z-m-1} \\ Z_{M+1}^{(n)} &= \frac{(z-1)!}{2} \sum_{i=0}^{z-1} [(3^n-1)(i+1) + (3^n+1)(z-i)] (Y_{M-1}^{(n)})^m (Z_{M-1}^{(n)})^{z-m-1} \end{aligned} \quad (9)$$

We now set $W_M = Y_M^{(n)}/Z_M^{(n)}$, extending [2, , eq. 4.9] into the recurrence relation

$$W_{M+1} = f_{n,z}(W_M) = \frac{\sum_{i=0}^{z-1} (3^n(z+1) + 2i + 1 - z) W_M^i}{\sum_{i=0}^{z-1} (3^n(z+1) - 2i - 1 + z) W_M^i} \quad (10)$$

² Note that, since Y_M and Z_M are initially defined for a branch adjoining the origin, i.e. with an ‘‘odd’’ root vertex at depth 1, using them in reference to a branch with a root vertex at depth 2, by altering the parity of the vertices, implicitly inverts the boundary conditions. We will rectify this by letting the branch B_M terminate in $|\uparrow\rangle$, and have an odd-parity root vertex, if M is even or the number of decorations n is odd, and terminate in $|\downarrow\rangle$ if M is odd and n is even.

Accounting for all of the decorations on the inward-reaching edge allows us to use, without modification, the equation in [1, following 4.11][2] for the polarization of the central spin:

$$\frac{\langle \Psi_M | S_z^{(0)} | \Psi_M \rangle}{\langle \Psi_M | \Psi_M \rangle} = \frac{\sum_{i=0}^z (z/2 - i) W_M^i}{\sum_{i=0}^z W_M^i} \equiv m_z(W_M). \quad (11)$$

In particular, we note that m_z is monotonic decreasing, with $m_z(0) = z/2$, $m_z(1) = 0$, and $m_z(\infty) = -z/2$.

A. Consequences of the recurrence relation

Much as observed by AKLT in the bare case, the basic key features of $f_{n,z}$ are that it is monotonic nondecreasing (for $0 \leq W \leq \infty$) and that $W = 1$ is a fixed point. We also note that it is manifestly true from the spin-flip-invariance of the system, which exchanges the variables Y and Z defined in (3), (4), that $f_{n,z}(W^{-1}) = f_{n,z}(W)^{-1}$. With the additional datum that

$$f_{n,z}(0) = \frac{3^n(z+1) - z + 1}{3^n(z+1) + z - 1} > 0,$$

we may conclude that:

1. Antiferromagnetic order corresponds to the existence of a fixed point of $f_{n,z}$ at some $0 \leq W_0 < 1$.
2. In order to establish that $W = 1$ is the unique (nonnegative) fixed point of $f_{n,z}$, it is necessary and sufficient to prove that $f(W) > W$ for all $0 < W < 1$.
3. When the fixed point $W = 1$ is unstable, i.e. $f'(W) > 1$, it is necessarily true that $f(W) < W$ in some neighborhood $(1 - \varepsilon, 1)$, and therefore there is at least one additional ordered, attractive fixed point.

With our rudimentary analysis, therefore, we will generally be able to conclusively prove the *existence* of antiferromagnetic order (without knowing the value of the fixed point, which corresponds to the value of the magnetization) but, in cases believed to be disordered, we will not be able to *disprove* the existence of such a fixed point.

Therefore, our guide to the behavior of the system is

$$f'_{n,z}(1) = \frac{z-1}{3^{n+1}}. \quad (12)$$

This suggests the absence of order when $z < 3^{n+1} + 1$ and implies the presence of order when $z > 3^{n+1} + 1$.

We now consider the marginal case $z = 3^{n+1} + 1$. As the denominator of (10) is positive-definite (with a value of $3^n z(z+1)$ at $W = 1$), we may determine the leading-order behavior of $f_{n,z}(1 - \varepsilon) - (1 - \varepsilon)$ (for $\varepsilon \equiv 1 - W$ small) expanding the numerator:

$$\begin{aligned} & \sum_{i=0}^{z-1} (3^n(z+1) + 2i + 1 - z)(1 - \varepsilon)^i - \sum_{i=0}^{z-1} (3^n(z+1) - 2i - 1 + z)(1 - \varepsilon)^i \\ & \simeq \frac{z(z+1)}{3}(3^{n+1} - z + 1)\varepsilon - \frac{z(z^2 - 1)}{6}(3^{n+1} - z + 1)\varepsilon^2 + \frac{z(z^2 - 1)(z - 2)}{60}(10 \times 3^n - 3z + 4)\varepsilon^3 \end{aligned} \quad (13)$$

In particular, when $z = 3^{n+1} + 1$ the first two terms vanish, and (substituting for $(z - 1)/3$ for 3^n) the sub-leading-order behavior of $f_{n,z}$ is

$$f_{n,z}(W) - W \simeq \frac{(1 - W)^3}{60}(z^2 - 4) > 0 \quad (14)$$

for $1 - W > 0$ small.

B. Asymptotic behavior

We first state the leading-order behavior of (11):

$$m_z(1 - \varepsilon) \simeq \frac{1}{z+1} \sum_{i=0}^z \left(\frac{z}{2} - i \right) (1 - i\varepsilon) = \frac{z(z+2)}{12}\varepsilon. \quad (15)$$

From (12), we can determine the asymptotic behavior of W_M for the disordered case $z < 3^{n+1} + 1$ (at least, assuming that there are no unexpected fixed points):

$$\begin{aligned} f_{n,z}(1 - \varepsilon) & \simeq 1 - \frac{z-1}{3^{n+1}}\varepsilon \\ 1 - W_M & \sim \left(\frac{z-1}{3^{n+1}} \right)^M \\ m_z(W_M) & \sim \left(\frac{z-1}{3^{n+1}} \right)^M. \end{aligned} \quad (16)$$

In other words, we may say there is an effective correlation length, of sorts, $\xi^{-1} = (n+1) \ln 3 - \ln(z-1)$.

Moving to the marginal case $z = 3^{n+1} + 1$, we note the following: If a function g has leading-order behavior $g(\varepsilon) = 1 - C\varepsilon^r + \mathcal{O}(\varepsilon^{r+1})$ for some coefficient C and exponent $r \geq 2$, it can be shown that

$$g\left(\frac{1}{r^{-1}\sqrt{(r-1)CM}}\right) = \frac{1}{r^{-1}\sqrt{(r-1)C(M+1)}} + \mathcal{O}(M^{-\frac{r}{r-1}}).$$

In particular, we may use the leading-order expansion in (14): for $g(1 - W) \equiv 1 - f_{n,z}(W)$, which is to say $r = 3$ and $C = \frac{z^2-4}{60}$ in the ansatz for g , we determine that the large-radius behavior of our order parameter will be governed by

$$\begin{aligned} W_M &\simeq 1 - \sqrt{\frac{30}{(z^2 - 4)M}} \\ m_z(W_M) &\simeq \frac{z}{2} \sqrt{\frac{z+2}{z-2} \times \frac{5}{6M}}. \end{aligned} \tag{17}$$

For the undecorated case, when $z = 4$, this becomes $m_z(W_M) \simeq \sqrt{\frac{10}{M}}$.

C. Numerical confirmation

Due to the inherent tensor-network “valence bond state” structure of the AKLT state and the loop-free nature of the Bethe lattice, when z is sufficiently small it is easy to directly compute the value of the Néel order parameter m_z and other observables on finite-size subsystems. We do so as follows:

- i. We take a “boundary state”, a one-qubit density matrix ρ_m initialized to $\rho_0 = |\uparrow\rangle\langle\uparrow|$.
- ii. We apply a generalization of the transfer matrix for degree z , constructed by contracting the spin- $z/2$ projector along its physical index and then contracting the final virtual index of both with singlet states. This operator, which we call \mathbb{E}_z and which matches the superoperator $\hat{\mathbb{E}}$ defined in [3, , eq. 1.3] is a superoperator that acts on operators on $z-1$ qubits (by contraction with the first $z-1$ virtual indices of the projectors) and produces an operator on a single qubit. This produces $\tilde{\rho}_{m+1} \equiv \mathbb{E}_z(\rho_m \otimes \cdots \otimes \rho_m)$.
- iii. We apply the 1D AKLT transfer matrix \mathbb{E}_2 n times to ρ_m (incorporating a line of decorations), yielding the next-level boundary state $\rho_{m+1} \equiv \mathbb{E}_2^n \tilde{\rho}_{m+1}$.
- iv. To evaluate the expectation value of an operator O acting on the central site of the radius- M system, we contract O with the physical indices of the spin- $z/2$ projector and its conjugate and then contract the virtual indices with z copies of ρ_M . (This yields $\langle \Psi_M | O | \Psi_M \rangle$ for the non-normalized state Ψ_M ; to normalize we perform the same contraction, but omitting O and directly contracting the physical indices of the projectors, to obtain $\langle \Psi_M | \Psi_M \rangle$.)

This procedure is a somewhat generalized version of that outlined in Fig. 2.

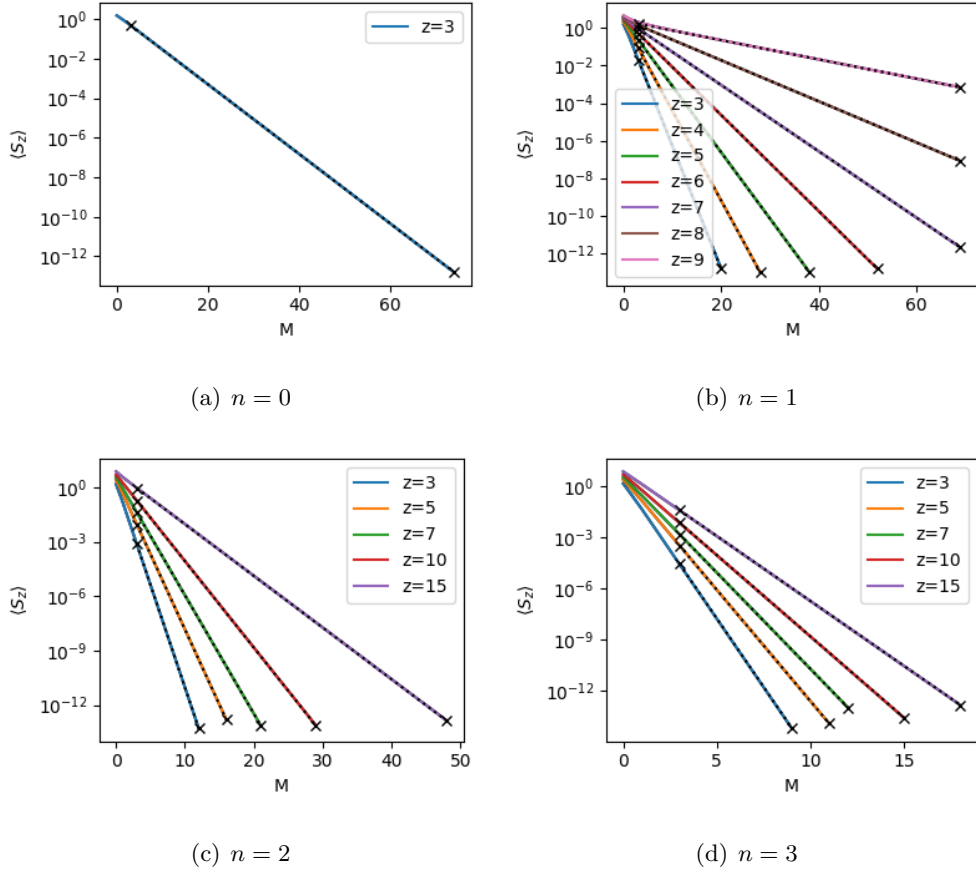


FIG. 3. Decay of the Néel order parameter for various numbers of decorations, within the disordered phase, calculated with tensor-network methods. The asymptotic behavior dictated by (16) is plotted with dotted lines and \times markers.

For confirmation of the recurrence relation (10), we will calculate values of m_z using (10) and (11) and plot those on top of the tensor-network calculations described above. (Since both calculations are exact, the lines will not be distinguishable). When $z \gtrsim 20$, these naïve tensor-network calculations are no longer practical, and we will instead only use direct calculation from (10).

In Fig. 3 we compare the large- M behavior of the Néel order parameter to that predicted by (16). In Fig. 4, we confirm the prediction that the state is antiferromagnetically ordered when $z > 3^{n+1} + 1$: in particular, the Néel order parameter converges to a nonzero expectation value. In Fig. 5, we confirm the power-law relation of (17) for the critical case $z = 3^{n+1} + 1$ for several values of z .

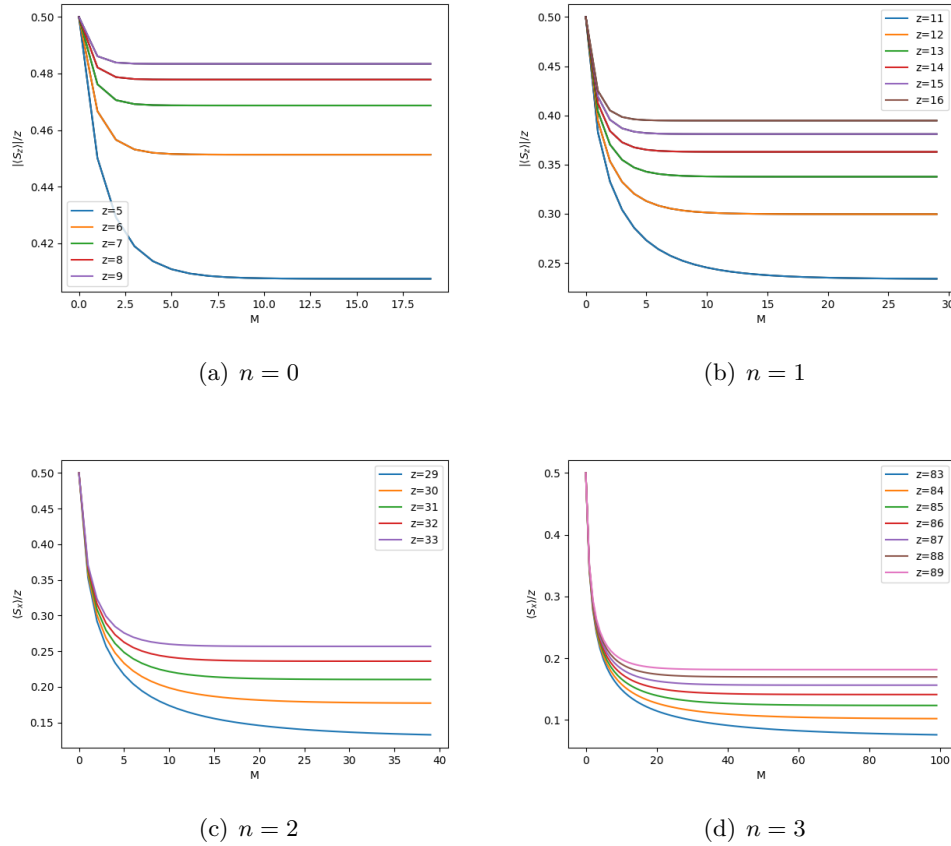


FIG. 4. Behavior of the Néel order parameter in the ordered phase. For (a) and (b) we use direct tensor-network calculations; for (c) and (d), order does not occur in cases where tensor-network computations are practical and so we use repeated application of the function $f_{n,z}$ instead.

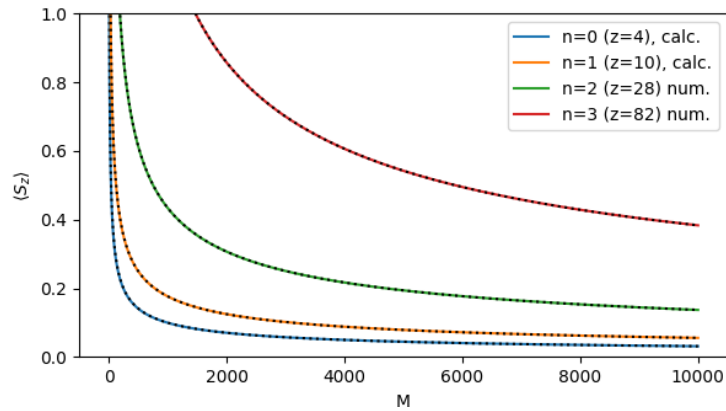


FIG. 5. Behavior of the Néel order parameter at the phase boundary, with computed values compared with the theoretical asymptotic behavior predicted in (17) (dotted). When this cannot be probed with naïve tensor-network calculations ($n > 1$), computation using (29) is used instead.

III. THE INFINITE STATE AND THE LOOP OPERATOR

In the predictions of (16) and (17), we have made use of the finite-size “Néel order parameter” of [2] to, for example, diagnose a distinction between “critical” behavior with infinite “correlation length” and a more conventional disordered AKLT phase with finite “correlation length”. One may pose a reasonable objection to this distinction that it is incompatible with taking the thermodynamic limit: that is, the behavior in question is seen across length scales equal to the system size, and so the possibility that it is due to finite-size effects has not been excluded. We will therefore briefly introduce a means of diagnosing these distinctions using the infinite state, which can be defined for any fixed-point boundary condition.

To summarize how this state is defined, we use the superoperators \mathbb{E}_2 and \mathbb{E}_z defined above, with which we can define the constraint on a pair of steady-state boundary density matrices ρ_∞^\pm as

$$\begin{aligned}\rho_\infty^+ &\propto \mathbb{E}_2^n \circ \mathbb{E}_z(\rho_\infty^- \otimes \cdots \otimes \rho_\infty^-) \\ \rho_\infty^- &\propto \mathbb{E}_2^n \circ \mathbb{E}_z(\rho_\infty^+ \otimes \cdots \otimes \rho_\infty^+)\end{aligned}\tag{18}$$

(We require a pair of density matrices due to the antiferromagnetic nature of the AKLT state; when the system is disordered, or when n is odd and thus the spin-1 decorations mediate an effectively ferromagnetic interaction between the “main” spin- $z/2$ sites, we expect $\rho_\infty^+ = \rho_\infty^-$.)

In particular, we may conclude that, for W_∞ a fixed point of the recurrence relation (10),

$$\rho_\infty^\pm \equiv \rho_z(W^{\pm 1}) \equiv \frac{1}{W_\infty^{1/2} + W_\infty^{-1/2}} \begin{pmatrix} W_\infty^{\mp \frac{1}{2}} & 0 \\ 0 & W_\infty^{\pm \frac{1}{2}} \end{pmatrix}\tag{19}$$

satisfies (18), as a consequence of our derivation of (10). (That is, they are defined by a ratio of eigenvalues W_∞ .) For all values of z and n , this means we can define a disordered steady state $\rho_0 = \frac{1}{2}\mathbb{1}$ from the trivial fixed point $W = 1$. When there is an additional fixed point $0 \leq W_A < 1$ representing antiferromagnetic order, this gives us an additional boundary steady state – or rather, applying $SU(2)$ transformations, an infinite family thereof.

Having established a boundary steady state, we can define a reduced density matrix \mathfrak{A}_M on a disc of radius M as follows: we simply take the AKLT construction on this disc and its conjugate and contract their free indices pairwise with ρ_∞^s (where s is the sign $(-1)^M$), and then normalize. Then the expectation value $\langle O \rangle_\infty$ of an operator O with finite support can be defined by taking the follows. By definition, there is some M such that the support of O is contained within the disc of radius M . Thus, we state that

$$\langle O \rangle_\infty = \text{tr}(\mathfrak{A}_M O).$$

We note that the construction of \mathfrak{A}_M can be applied to boundary density matrices which are not steady states, and define a (reduced) density matrix $\mathfrak{B}_M(\rho)$, such that

$$\mathfrak{B}_M(\rho_\infty^{(-1)^M}) = \mathfrak{A}_M.$$

This is similar to the construction used above to explicitly calculate the Néel order parameter; in particular,

$$m_z(W_M) = (-1)^M \text{tr} \left(\mathfrak{B}_M (|\uparrow\rangle\langle\uparrow|) S_z^{(0)} \right) = (-1)^{M-N} \text{tr} \left(\mathfrak{B}_{M-N}(\rho_z(W_N)) S_z^{(0)} \right).$$

With the infinite state defined, we will introduce the operator we will use to diagnose long-range behavior. For a more physical setting than the Bethe lattice, we might use a simple two-point correlator; however, as noted in [2] these will display exponential decay regardless of order. Instead, we simulate the kind of boundary conditions we have been using to diagnose decay with a loop operator defined as

$$L_M(\vec{r}) = \prod_{p \text{ at radius } M} \exp((-1)^{(n+1)M} \vec{r} \cdot \vec{S}^{(p)}), \quad (20)$$

where \vec{r} is some three-element vector and $\vec{S}^{(p)}$ is the operator-valued vector $S_x \hat{x}^{(p)} + S_y \hat{y}^{(p)} + S_z \hat{z}^{(p)}$ acting on some (degree- z) site p . (The sign is inserted for consistency). To analyze the behavior of the system when such an operator is applied, we first see how the expressions in (7) are modified when the physical index is contracted with $\exp(-(-1)^{(n+1)M} \tau S_z)$:

$$\begin{aligned} Y_1^{(0)} &= (z-1)! \sum_{m=0}^{z-1} (m+1) e^{-\tau(m+1-z/2)} (Y_0^{(n)})^m (Z_0^{(n)})^{z-m-1} \\ &= (z-1)! e^{-\tau(z/2+1)} (Z_0^{(n)})^z \sum_{m=0}^{z-1} (m+1) (e^{-\tau} W_0^{(n)})^m \\ Z_1^{(0)} &= (z-1)! \sum_{m=0}^{z-1} (z-m) e^{-\tau(m-z/2)} (Y_0^{(n)})^m (Z_0^{(n)})^{z-m-1} \\ &= (z-1)! e^{-\tau z/2} (Z_0^{(n)})^z \sum_{m=0}^{z-1} (z-m) (e^{-\tau} W_0^{(n)})^m. \end{aligned} \quad (21)$$

In other words, the relationship between $W_0^{(n)}$ and $W_1^{(0)}$, which normally is given by the “bare-lattice” recurrence relation $W_1^{(0)} = f_{0,z}(W_1^{(n)})$, is instead given by $W_1^{(0)} = e^{-\tau} f_{0,z}(e^{-\tau} W_1^{(n)})$. We can therefore capture the effect of the loop operator on the parameter W with

$$W \mapsto \tilde{f}_{n,z}(W, \tau) = f_{0,2^n}(e^{-\tau} f_{0,z}(e^{-\tau} W)). \quad (22)$$

This does not give us immediate information on expectation values involving $L_M(\tau \hat{z})$, since the process of deriving those recurrence relations involves implicit normalization. Nonetheless the

construction of the density matrix $\text{tr}_M(L_M(\tau\hat{z})\mathcal{A}_M)$ (where we have performed a partial trace over the physical indices on sites at radius M as well as those on the decorations on segments connecting to those sites), once normalized, proceeds identically to the construction of $\mathfrak{B}_{M-1}(\tilde{\rho})$, with $\tilde{\rho} \equiv \rho_z(\tilde{f}_{n,z}(W_\infty, \tau))$. We therefore conclude that, for an operator O supported within radius M ,

$$\langle L_M(\tau\hat{z})O \rangle_\infty = \text{tr}(\mathfrak{B}_M(\tilde{\rho})O) \langle L_M(\tau\hat{z}) \rangle_\infty. \quad (23)$$

In particular, while the behavior of $\langle L_M(\tau\hat{z}) \rangle$, and therefore of $\langle L_M(\tau\hat{z})O \rangle$, will typically be dominated by short-range effects due to the exponential scaling $z(z-1)^{M-1}$ of the number of sites at radius M in the Bethe lattice, we can effectively isolate long-range effects of the loop operator with the functional

$$L_{M,\vec{r}}[O] \equiv \frac{\langle L_M(\vec{r})O \rangle_\infty}{\langle L_M(\vec{r}) \rangle_\infty} = \text{tr}(\mathfrak{B}_M(\tilde{\rho})O) \quad (24)$$

(with the latter equality in the case of $\vec{r} = \tau\hat{z}$). We will call this the *loop expectation value*. As an example, we will use this to demonstrate critical decay in Fig. 7.

As a final note, we may use these loop operators to more precisely infer the behavior of two-point functions. In the small- τ limit, we may generally represent $\tilde{f}_{n,z}(W_\infty, \tau)$ as a small correction with first-order behavior $W_\infty - \alpha\tau$. Since we already know the leading-order behavior of $f_{n,z}$ and m_z in the disordered case $W_\infty = 1$, we may conclude from (15) and (16) that

$$L_{M,\tau\hat{z}}[S_z^{(0)}] \simeq \alpha\tau \frac{z(z+1)}{3} \left(\frac{z-1}{3^{n+1}} \right)^M \sim \tau e^{-M/\xi}.$$

(We include the cases where $W = 1$ is a marginal or unstable fixed point, in which $\xi = \infty$ and $\xi < 0$ respectively.) In the same limit, the loop operator, being a product of exponentials in τ , is straightforward to expand to first order:

$$L_M(\tau\hat{z}) = 1 - (-1)^{(n+1)M} \tau \sum_{p \text{ at radius } M} S_z^{(p)} + \mathcal{O}(\tau^2).$$

Since, again confined to the disordered state where $W = 1$, one-point functions vanish, this implies that the loop expectation value behaves as

$$L_{M,\tau\hat{z}}[S_z^{(0)}] = 1 - (-1)^{(n+1)M} \tau \sum_{p \text{ at radius } M} \langle S_z^{(0)} S_z^{(p)} \rangle_\infty.$$

Equating these two approximations, and noting that the symmetry of the Bethe lattice implies that the above two-point function will be identical for any p , we find

$$\lim_{\tau \rightarrow 0} \tau^{-1} L_{M,\tau\hat{z}}[S_z^{(0)}] = -(-1)^{(n+1)M} z(z-1)^{M-1} \langle S_z^{(0)} S_z^{(p)} \rangle_\infty = \alpha \frac{z(z+1)}{3} e^{-M/\xi},$$

and therefore,

$$\langle S_z^{(0)} S_z^{(p)} \rangle_\infty = -(-1)^{(n+1)M} \alpha \frac{z^2 - 1}{3} e^{-(1/\xi + \log(z-1))M}. \quad (25)$$

Note that the actual form of the effective correlation length

$$\xi'^{-1} = \xi^{-1} + \log(z-1) = (n+1) \log 3$$

provides a re-derivation of the trivial prediction found in [2], i.e. a two-point function that (in the undecorated case) decays as 3^{-M} . However, we can still use this to conclude that, for Bethe lattice systems of degree z more generally, with O some order parameter of spontaneously-broken symmetry, if

$$\langle O^{(0)} O^{(p)} \rangle \sim e^{-M/\xi'}, \quad \begin{cases} \xi'^{-1} > \log(z-1) \Rightarrow \text{disorder,} \\ \xi'^{-1} = \log(z-1) \Rightarrow \text{criticality, and} \\ \xi'^{-1} < \log(z-1) \Rightarrow \text{order.} \end{cases} \quad (26)$$

Additionally, when the system is in an ordered configuration with polarization $m_0 = m_z(W_\infty)$, we can expect – again for M large but fixed –

$$\begin{aligned} m_z(f_{n,z}^M(W_\infty + \alpha\tau)) &\simeq m_0 + \alpha\tau e^{-M/\xi_A} \\ \langle L_M(\tau\hat{z}) S_z^{(0)} \rangle_\infty &\simeq \langle S_z^{(0)} \rangle_\infty - (-1)^{n(M+1)} z(z-1)^{M-1} \tau \langle S_z^{(0)} S_z^{(p)} \rangle_\infty \\ \langle L_M(\tau\hat{z}) \rangle_\infty &\simeq 1 - (-1)^{n(M+1)} z(z-1)^{M-1} \tau \langle S_z^{(p)} \rangle_\infty \\ L_{M,\tau\hat{z}}[S_z^{(0)}] &\simeq m_0 - (-1)^{n(M+1)} z(z-1)^{M-1} \tau (\langle S_z^{(0)} S_z^{(p)} \rangle_\infty - m_0^2) \\ \langle S_z^{(0)} S_z^{(p)} \rangle_\infty &\simeq m_0^2 - \frac{z-1}{z} \alpha e^{-M(1/\xi_A + \log(z-1))}, \end{aligned} \quad (27)$$

where the effective correlation length ξ_A , though in practice difficult to calculate analytically, is defined by $\xi_A^{-1} = 1 - f'_{n,z}(W_\infty)$.

IV. INTERPOLATING n

We have, in (12), an appealingly simple criterion for the presence of order: a line $3^{n+1} = z - 1$ separating order and disorder in all cases. Indeed, we find that nearly all the expressions we have used to determine the behavior of these decorated systems have a rational dependence on 3^n . Therefore, if we could somehow make the parameter $\Gamma = 3^n$ continuous, we would expect a phase transition for any $z > 4$ at the critical point

$$\Gamma = \frac{z-1}{3}.$$

Instead of using this parameter Γ , we will find it more practical to employ a parameter³

$$\begin{aligned}\gamma &\equiv \frac{\Gamma - 1}{\Gamma + 1} = \frac{3^n - 1}{3^n + 1}, \text{ or} \\ 3^n &= \frac{1 + \gamma}{1 - \gamma}.\end{aligned}\tag{28}$$

This allows us to rewrite (10) as

$$f_{\gamma,z}(W) = \frac{\sum_{i=0}^{z-1} [(z-i)\gamma + (i+1)] W^i}{\sum_{i=0}^{z-1} [(i+1)\gamma + (z-i)] W^i}.\tag{29}$$

The two methods we use to reproduce this, in part or in whole, are detailed below.

A. A deformed decoration

We may seek to emulate (8) by directly modifying (7). The coefficients applied to $(Y^{(k-1)}, Z^{(k-1)})$ there come directly from elements of the spin-1 projector. Modifications made to this object with an onsite deformation much like those studied in [10–12]. In particular, a diagonal (in the z basis deformation will alter (6) by multiplication on the appropriate term (by the square of element in question). Thus, with a single decorated, deformed with a matrix defined by (real) diagonal elements $(1, a, 1)$, (8) becomes

$$\begin{pmatrix} Y_M^{(1)} \\ Z_M^{(1)} \end{pmatrix} = \begin{pmatrix} 2 & a^2 \\ a^2 & 2 \end{pmatrix} \begin{pmatrix} Y_M^{(0)} \\ Z_M^{(0)} \end{pmatrix}.$$

Referring again to (8), the desired matrix in this expression would be proportional to

$$\begin{pmatrix} \frac{3^n+1}{2} & \frac{3^n-1}{2} \\ \frac{3^n-1}{2} & \frac{3^n+1}{2} \end{pmatrix} = \frac{3^n+1}{4} \begin{pmatrix} 2 & 2\gamma \\ 2\gamma & 2 \end{pmatrix},\tag{30}$$

which is to say that we can achieve the behavior in (29) by deforming the $m_z = 0$ index of a single decoration by $a = \sqrt{2\gamma}$.

B. Interpolating a single decoration

A deformation like the one used above explicitly breaks the $SU(2)$ down to $O(2)$. We will explore the consequences of doing so later, but for now we will seek a way of replicating this behavior that is $SU(2)$ -invariant.

³ There are various reasons for using γ over the more obvious Γ ; it will simplify some equations and make the “antiferromagnetic-ferromagnetic” duality that will arise much simpler. For now we will simply say that the “bare” case $\gamma = 0$ ($\Gamma = 1$) is a much firmer boundary than the “decoupling” point $\gamma = 1$ ($\Gamma \rightarrow \infty$).

In order to do so, we analyze the (full) transfer matrices on the decorated edge. In a basis $(|\uparrow\rangle\langle\uparrow|, |\uparrow\rangle\langle\downarrow|, |\downarrow\rangle\langle\uparrow|, |\downarrow\rangle\langle\downarrow|)$ for the boundary density matrices, we can write the transfer matrix of a single decoration as $s_2 A_2 s_2$, where

$$s_2 = \begin{pmatrix} 0 & 0 & 0 & 1 \\ 0 & 0 & -1 & 0 \\ 0 & -1 & 0 & 0 \\ 1 & 0 & 0 & 0 \end{pmatrix}$$

is the tensor product of two singlet states and

$$A = \begin{pmatrix} 1 & 0 & 0 & \frac{1}{2} \\ 0 & 0 & \frac{1}{2} & 0 \\ 0 & \frac{1}{2} & 0 & 0 \\ \frac{1}{2} & 0 & 0 & 0 \end{pmatrix}$$

is the result of contracting two spin-1 projectors.

In this basis, s_2 and A_2 commute,⁴ and so the transfer matrix for n decorations may be written

$$(s_2 A_2)^n s_2 = A_2^n s_2^{n+1}.$$

Blockwise analysis of A_2 and s_2 leads us to conclude

$$A_2^n = \frac{1}{2^{n+1}} \begin{pmatrix} 3^n + 1 & 0 & 0 & 3^n - 1 \\ 0 & 1 + (-1)^n & 1 - (-1)^n & 0 \\ 0 & 1 - (-1)^n & 1 + (-1)^n & 0 \\ 3^n - 1 & 0 & 0 & 3^n + 1 \end{pmatrix} \quad (31)$$

$$A_2^n s_2^{n+1} = \frac{1}{2^{n+1}} \begin{pmatrix} 3^n - (-1)^n & 0 & 0 & 3^n + (-1)^n \\ 0 & 0 & 2(-1)^{n+1} & 0 \\ 0 & 2(-1)^{n+1} & 0 & 0 \\ 3^n + (-1)^n & 0 & 0 & 3^n - (-1)^n \end{pmatrix} \quad (32)$$

Crucially, these transfer matrices span a two-dimensional real space. We should therefore be able to obtain those by combining the $n = 0$ and $n = 1$ cases, using a ‘‘perturbation’’ parameter δ^2 and

⁴ We note that we must use caution when treating s_2 and A_2 as endomorphisms or square matrices; rather than both belonging to $\text{Hom}(V, V) \cong V \otimes V^*$, they belong to $V \otimes V$ and $V^* \otimes V^*$, respectively, with V being the $1/2 \otimes 1/2^*$ representation of $SU(2)$.

an unstated normalization factor:

$$s_2 + \delta^2 s_2 A_2 s_2 = \begin{pmatrix} \delta^2 & 0 & 0 & \frac{\delta^2}{2} + 1 \\ 0 & 0 & \frac{\delta^2}{2} - 1 & 0 \\ 0 & \frac{\delta^2}{2} - 1 & 0 & 0 \\ \frac{\delta^2}{2} + 1 & 0 & 0 & \delta^2 \end{pmatrix} \propto \begin{cases} \frac{3^n+1}{2^{n+1}} \begin{pmatrix} \gamma & 0 & 0 & 1 \\ 0 & 0 & \gamma-1 & 0 \\ 0 & \gamma-1 & 0 & 0 \\ 1 & 0 & 0 & \gamma \end{pmatrix}, & n \text{ even} \\ \frac{3^n+1}{2^{n+1}} \begin{pmatrix} 1 & 0 & 0 & \gamma \\ 0 & 0 & 1-\gamma & 0 \\ 0 & 1-\gamma & 0 & 0 \\ \gamma & 0 & 0 & 1 \end{pmatrix}, & n \text{ odd} \end{cases} \quad (33)$$

Combining a single decoration with the undecorated edge has the effect of frustrating the antiferromagnetic AKLT interactions; in particular we expect an antiferromagnetic system for $\delta \ll 1$ and a ferromagnetic system for $\delta \gg 1$. We can then establish two correspondences:

$$\delta^2 = \begin{cases} \frac{2\gamma}{2-\gamma}, & n \text{ even} \\ \frac{2}{2\gamma-1}, & n \text{ odd} \end{cases}. \quad (34)$$

1. The ferromagnetic-antiferromagnetic “duality”

It is of some interest that the two expressions in (34) are related to one another by the exchange $\gamma \leftrightarrow \gamma^{-1}$. Looking to (29), we realize that

$$f_{\gamma^{-1},z}(W) = f_{\gamma,z}(W^{-1}) = f_{\gamma,z}(W)^{-1}.$$

That is, this relation interchanges an alternating polarization with a monotonic one. (Since f is based on the AKLT-norm formula (1) which flips the spin orientation on alternating sites, the former actually represents ferromagnetic interactions and the latter antiferromagnetic, at least for $n = 0$. Since the unperturbed case in the frustration method of realizing continuous γ is $n = 0$, whereas the unperturbed case in the deformation method is $n = 1$, we will consider the antiferromagnetic regime to be $\gamma < 1$ in the former case and $\gamma > 1$ in the latter, a choice which could not possibly lead to any confusion.)

This is related to the fact that the derivation of this transfer matrix, and the various other expressions related to z -polarization we have used, effectively only rely on the elements acting on $\{|\uparrow\rangle\langle\uparrow|, |\downarrow\rangle\langle\downarrow|\}$ (or, in terms of (1), cases where $G = G'$). When we are considering observables diagonal in the z basis acting on states that are disordered or $\pm z$ -polarized, this means that expectation values can be exactly mapped onto one another under this “duality”, after flipping spin

orientations on alternating sites. Due to $SU(2)$ invariance, we can do this with states and observables of any single polarization. Simple arguments will show that a few additional observables, such as $\langle \vec{r} \cdot \vec{S} \rangle$, can be related in this way (as the contribution from the component of \vec{r} perpendicular to the direction of polarization will vanish), but there is no more general duality. Nonetheless, we will make our default choice of correspondence

$$\delta^2 = \frac{2\gamma}{2 - \gamma},$$

such that $\gamma < 1$ is antiferromagnetic and $\gamma > 1$ ferromagnetic, and such that the correspondence with the original n -times decorated system is incomplete when n is odd.

We further take note of the special “self-dual” case $\gamma = 1$, corresponding to the $n \rightarrow \infty$ limit. Due to the finite correlation length of the AKLT chain, we would expect this to act to decouple otherwise-neighboring Bethe lattice spins, and we can demonstrate that this is the case. Generally, we can treat the decoration as a mapping from a pair of virtual spins to a singlet-triplet space $\text{span}\{|s\rangle, |-\rangle, |0\rangle, |+\rangle\}$, equal to

$$|0\rangle (\langle \uparrow\downarrow | - \langle \downarrow\uparrow |) + \delta |+\rangle \langle \downarrow\downarrow | + \delta |-\rangle \langle \uparrow\uparrow | - \delta \sqrt{1/2} |0\rangle (\langle \uparrow\downarrow | + \langle \downarrow\uparrow |).$$

Then, when $\gamma = 1$ and so $\delta = \sqrt{2}$, this is proportional to a unitary transformation. Therefore, this effectively decouples the order- z spins from each other.

C. The phase transition

As alluded to above, realizing (29) yields a transition at $\Gamma_c = (z - 1)/3$, or

$$\gamma_c = \frac{z - 4}{z + 2}.$$

(We note that this also implies, by the ferromagnetic-antiferromagnetic “duality” we have just introduced, another transition at $\gamma = (z + 2)/(z - 4)$.)

At this critical point we find that the leading-order behavior is still governed by the power-law decay in (17), as we confirm in Fig. 7.

Given the presence of a continuous parameter, we may determine some additional critical exponents. First, in the disordered phase, i.e. when $\gamma_c < \gamma < 1$, we can rephrase (16) as the presence of a sort of correlation length: noting that the asymptotic behavior can be written $m_z \sim (\Gamma_c/\Gamma)^M$, we determine

$$\xi^{-1} = \log(1 + \gamma) - \log(1 - \gamma) - \log(1 - \gamma_c) + \log(1 + \gamma_c) \simeq \frac{2}{1 - \gamma_c^2} (\gamma - \gamma_c) \quad (35)$$

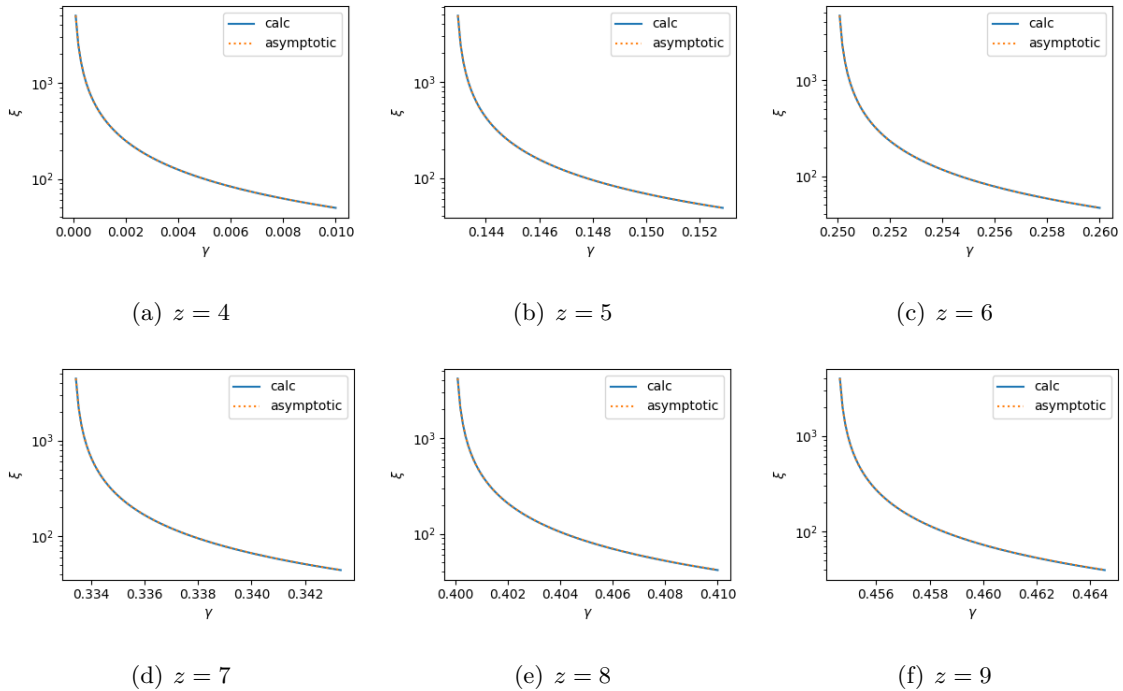


FIG. 6. The divergence of the correlation length ξ , with values computed directly from the recurrence relation (29), compared with the predicted asymptotic values (dotted) shown in (35).

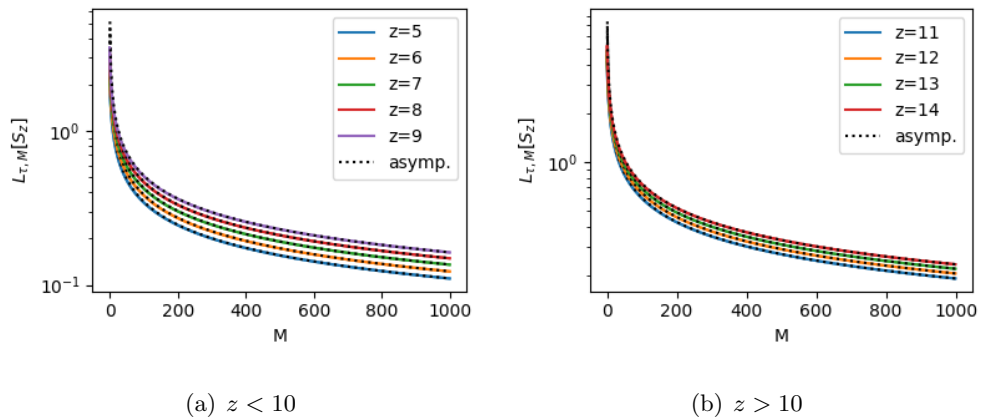


FIG. 7. Behavior of the “order parameter” (24), with $\tau = 1$, at the critical point for various z in cases not coinciding with integer n . Computations using both types of decoration are shown, but cannot be distinguished from each other; the asymptotic behavior in (17) is overlaid.

in the vicinity of the critical point: that is, as shown in 6, the correlation length diverges as $\xi \sim \Delta\gamma^{-1}$.

Meanwhile, we may now begin in earnest to study the behavior of the system within the ordered phase ($\gamma < \gamma_c$), since we may be able to determine the location of the attractive fixed point for

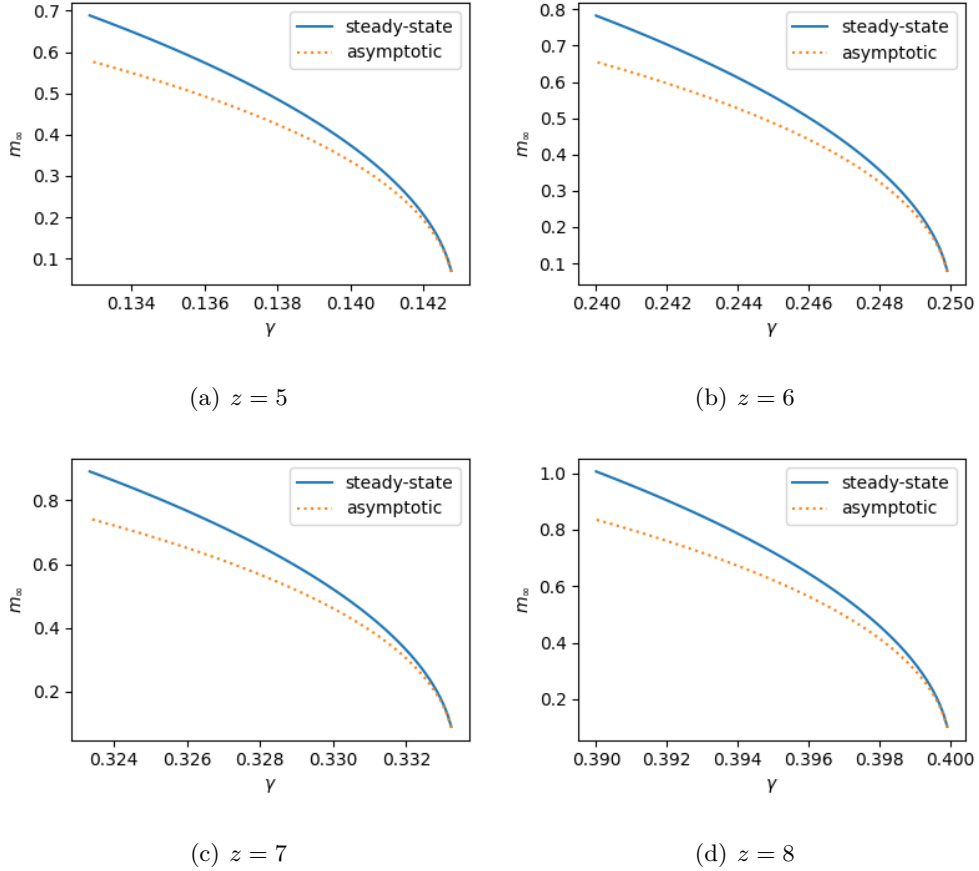


FIG. 8. Behavior of the steady-state magnetization ($\langle S_z \rangle$ for the z -polarized state) in the ordered phase near the critical point, for various values of z . We plot results from both realizations, from direct calculation with $f_{\Gamma,z}$, and with the approximation (36).

$\gamma_c - \gamma$ sufficiently small - at least, so long as γ_c is truly a second-order transition, as the critical behavior suggests. We analyze the ordered fixed point near the critical point using the third-order expansion (13) of the numerator of $f_{\gamma,z}(W) - W$, with $W = 1 - \varepsilon$ and $\Delta\gamma = \gamma - \gamma_c$ ($0 < -\Delta\gamma \ll 1$), replacing $3^{n+1} - z + 1$ for the time with $3\Delta\Gamma = \Delta\gamma^{(z+2)^2}/6$. Then the fixed point is approximately determined by $0 < \varepsilon \ll 1$ such that

$$z(z+1)\Delta\Gamma \varepsilon_c - z(z^2-1)\frac{\Delta\Gamma}{2}\varepsilon_c^2 + z(z^2-1)(z-2)\left[\frac{\Delta\Gamma}{6} + \frac{z+2}{180}\right]\varepsilon_c^3 = 0.$$

We solve this to get an approximation to the fixed point $W_\infty \simeq 1 - \varepsilon_c$, where

$$\varepsilon_c = \frac{45\Delta\Gamma + 6\sqrt{-5\frac{\Delta\Gamma}{z-1}}\sqrt{\frac{15}{4}(5z-13)\Delta\Gamma + z^2 - 4}}{(z-2)(30\Gamma + z + 2)} \quad (36)$$

$$\simeq 6(-\Delta\Gamma)^{1/2}\sqrt{\frac{5}{(z-1)(z^2-4)}} \simeq (\gamma_c - \gamma)^{1/2}\sqrt{\frac{10(z+2)}{(z-1)(z-2)}}. \quad (37)$$

We confirm this numerically in Fig. 8.

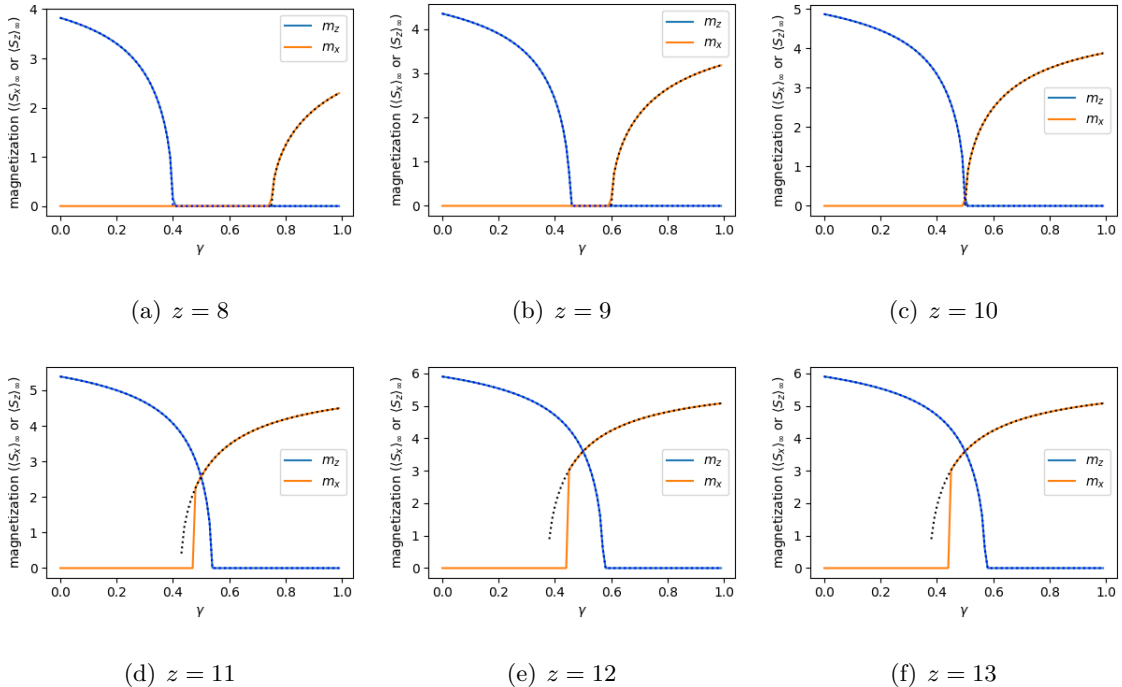


FIG. 9. Limiting values of the x and z magnetization for coordination numbers 8-13, for the anisotropic implementation of continuous γ . In $z = 11$ and $z = 12$, when approaching the x transition from the ordered side, we see an aberration due to spontaneous symmetry breaking, i.e. the system becomes polarized in the z direction and therefore loses polarization in the x direction.

V. COMPETING ORDER IN THE ANISOTROPIC REALIZATION

In subsection IV A, we realized the recurrence relation (29) by deforming the AKLT state on the singly-decorated Bethe lattice. Unlike the realization in subsection IV B, this breaks the $SU(2)$ symmetry of the AKLT state down to the $O(2)$ subgroup (generated by arbitrary rotations about the z axis and the π rotation about, e.g., the x axis.) The conclusions we obtained from this analysis determine when we observe magnetic polarization of along the symmetry axis, spontaneously breaking the \mathbb{Z}_2 quotient group; e.g., for coordination number $z > 10$, when the model with $n = 1$ isotropic decoration (corresponding to parameter $\gamma = 1/2$) exhibits spontaneous breaking of $SU(2)$, we find that we can tune γ up to a critical point γ_c above which the state is disordered, whereas for the case $z = 10$ where the isotropic model is critical, we find that spontaneous symmetry breaking occurs at any value $\gamma < 1/2$. It is natural, then, to ask when polarization in the basal xy plane occurs, particularly given that we know it does in the aforementioned isotropic $z > 10$ cases.

We will primarily consider polarization along a single axis within the xy plane: without loss of generality, the x axis. When we wish to examine the system in the presence of possible x

polarization, and/or under the action of some combination of S_x operators, we must restore the sum over the second subset G' in (1). That is, when we factor out branches of the Bethe lattice as in (3) and (4), we must consider factors, which I will label X_M^\pm , corresponding to the cases where $G \neq G'$ on the edge in question:

$$X_M^\pm = \sum_{G,G'} \delta_{m_0(G),m_0(G')\pm 1} c_z(m_0(G) + \frac{1\mp 1}{2}) \prod_{k \in B_M} \delta_{m_k(G),m_k(G')} c_z(m_k(G))$$

(where again $c_z(m) \equiv m!(z-m)!$ for convenience). Ultimately this leads us to rewrite (6), cataloging the possible options by numbers m set to equal $m_0(G)$, i.e. the total number of edges in G incident on the root vertex, and i set to equal the number of *pairs* of edges on which G and G' do not match:

$$\begin{aligned} Y_{M+1} &= \sum_{i=0}^{\lfloor z-1/2 \rfloor} \sum_{m=i}^{z-i-1} \binom{z-1}{m} \binom{m}{i} \binom{z-m-1}{i} (m+1)!(z-m-1)! Y_M^{m-i} Z_M^{z-m-i-1} (X_M^+)^i (X_M^-)^i \\ Z_{M+1} &= \sum_{i=0}^{\lfloor z-1/2 \rfloor} \sum_{m=i}^{z-i-1} \binom{z-1}{m} \binom{m}{i} \binom{z-m-1}{i} m!(z-m)! Y_M^{m-i} Z_M^{z-m-i-1} (X_M^+)^i (X_M^-)^i \\ X_{M+1}^+ &= \sum_{i=0}^{\lfloor z/2 \rfloor - 1} \sum_{m=i}^{z-i-2} \binom{z-1}{m} \binom{m}{i} \binom{z-m-1}{i+1} (m+1)!(z-m-1)! Y_M^{m-i} Z_M^{z-m-i-2} (X_M^+)^i (X_M^-)^{i+1} \\ X_{M+1}^- &= \sum_{i=0}^{\lfloor z/2 \rfloor - 1} \sum_{m=i+1}^{z-i-1} \binom{z-1}{m} \binom{m}{i+1} \binom{z-m-1}{i} m!(z-m)! Y_M^{m-i-1} Z_M^{z-m-i-1} (X_M^+)^{i+1} (X_M^-)^i. \end{aligned}$$

On the lattice with a single decoration deformed as above by a , we extend the remaining two equations from (7) by setting $z = 2$ and multiplying terms corresponding to $m_i = 1$ by $a^2 = 2\gamma$:

$$\begin{aligned} Y_M^{(1)} &= 2Y_M^{(0)} + 2\gamma Z_M^{(0)} \\ Z_M^{(1)} &= 2\gamma Y_M^{(0)} + 2Z_M^{(0)} \\ X_M^{\pm(1)} &= 2\gamma X_M^{\mp(0)} \end{aligned}$$

We have seen that reflection-invariance in the z direction is equivalent to $Y = Z$; we may also see that reflection-invariance in the y direction is equivalent to $X^+ = X^-$, and indeed, the above equations preserve these relations.

Then we can turn the above recursive equations into

$$\begin{aligned} Y_{M+1}^{(0)} &= \sum_{i=0}^{\lfloor z-1/2 \rfloor} (Y_M^{(1)})^{z-2i-1} (X_M^{(1)})^{2i} \sum_{m=i}^{z-i-1} \frac{(z-1)!(m+1)!(z-m-1)!}{i!^2(m-i)!(z-m-i-1)!} \\ X_{M+1}^{(0)} &= \sum_{i=0}^{\lfloor z/2 \rfloor - 1} (Y_M^{(1)})^{z-2i-2} (X_M^{(1)})^{2i+1} \sum_{m=i+1}^{z-i-1} \frac{(z-1)!m!(z-m)!}{i!(i+1)!(m-i-1)!(z-m-i-1)!} \\ Y_M^{(1)} &= 2(1+\gamma)Y_M^{(0)} \\ X_M^{(1)} &= 2\gamma X_M^{(0)}, \end{aligned}$$

or, defining a single parameter $V_M = X_M^{(1)}/Y_M^{(1)}$,

$$Y_{M+1}^{(1)} = 2(1+\gamma)(z-1)!(Y_M^{(1)})^{z-1} \sum_{i=0}^{\lfloor z-1/2 \rfloor} (i+1)V_M^{2i} \sum_{n=i}^{z-i-1} \binom{n+1}{i+1} \binom{z-n-1}{i}$$

$$X_{M+1}^{(1)} = 2\gamma(z-1)!(Y_M^{(1)})^{z-1} \sum_{i=0}^{\lfloor z/2 \rfloor - 1} (i+1)V_M^{2i+1} \sum_{n=i+1}^{z-i-1} \binom{n}{i+1} \binom{z-n}{i+1}$$

Taking the quotient, and applying a combinatorial identity, we obtain

$$V_{M+1}^{(1)} = \frac{(1+\gamma) \sum_{j=0}^z \frac{1+(-1)^j}{2} \frac{j+2}{2} \binom{z+1}{j+2} (V_M^{(1)})^j}{\gamma \sum_{j=0}^z \frac{1-(-1)^j}{2} \frac{j+3}{2} \binom{z+1}{j+2} (V_M^{(1)})^j},$$

which we can reduce with application of the binomial theorem and its derivative to

$$V \mapsto g_{\gamma,z}(V) = \frac{\gamma}{1+\gamma} \frac{(Vz-1)(1+V)^z + (1+Vz)(1-V)^z}{V(z+1)[(1+V)^z - (1-V)^z]}. \quad (38)$$

A. x -polarization in the isotropic system

We note that, in the isotropic case, we should be able to derive the behavior with $+x$ boundary conditions from the behavior with $+z$ boundary conditions. In particular we can apply to every degree of freedom the $SU(2)$ Hadamard transformation

$$H = \frac{1}{\sqrt{2}} \begin{pmatrix} 1 & 1 \\ 1 & -1 \end{pmatrix}.$$

As an object that transforms under $SU(2)$, the factors that we have been working with combine into a transfer matrix

$$\rho_M = \begin{pmatrix} Z_M & X_M^+ \\ X_M^- & Y_M \end{pmatrix}.$$

Then we relate the z -polarized conditions, $X^- = X^+ = 0$, to the x -polarized conditions, $X^- = X^+, Y = Z$, via

$$H \begin{pmatrix} Z & 0 \\ 0 & Y \end{pmatrix} H^\dagger = \begin{pmatrix} \frac{Y+Z}{2} & \frac{Z-Y}{2} \\ \frac{Z-Y}{2} & \frac{Y+Z}{2} \end{pmatrix},$$

which allows us to make the substitution

$$V \leftarrow \frac{1-W}{1+W}. \quad (39)$$

We can rewrite (29) in more closed form as

$$f_{z,\gamma}(W) = \frac{(1 + \gamma z) - \gamma(z + 1)W - (z + 1)W^z + (z + \gamma)W^{z+1}}{(z + \gamma) - (z + 1)W - \gamma(z + 1)W^z + (1 + \gamma z)W^{z+1}}.$$

Substituting $W \rightarrow \frac{1-V}{1+V}$,

$$\tilde{g}_{z,\gamma}(V) \equiv \frac{1 - f_{\gamma,z}(V+1/V-1)}{1 + f_{\gamma,z}(V+1/V-1)} = \frac{1 - \gamma}{1 + \gamma} \frac{1}{1 + z} \frac{(1 - zV)(1 + V)^z - (1 + zV)(1 - V)^z}{V(1 + V)^z - V(1 - V)^z} \quad (40)$$

When we compare (38) with (40), we find that the behavior of the deformed-decorated system with respect to the basal plane matches the behavior of the same system with respect to the symmetry axis for $\hat{\gamma}$ when

$$\begin{aligned} \frac{\gamma}{1 + \gamma} &= \frac{1 - \hat{\gamma}}{1 + \hat{\gamma}}, \text{ or} \\ \hat{\gamma} &= \frac{1}{1 + 2\gamma}. \end{aligned} \quad (41)$$

Of course, in the undeformed case $\gamma = 1/2$, the system is isotropic, $\hat{\gamma} = \gamma$. In particular, for $z = 10$ we see an order/disorder transition in both the basal plane and the symmetry axis at this value. More generally, however, we find that there are two transitions, γ_x and γ_z^5 , and

$$\gamma_x = \frac{1}{2\hat{\gamma}_z} - \frac{1}{2} = \frac{3}{z - 4}. \quad (42)$$

Note as well that this xy/z “duality” (41) maps the entire accessible⁶ range $[0, \infty]$ γ to $\hat{\gamma} \in [0, 1]$, meaning that these systems will not spontaneously order antiferromagnetically along the basal plane.

We therefore conclude that these systems have the following behaviors:

- For $z = 3$ there is no spontaneous symmetry breaking; in all cases the system should be disordered throughout both the “ferromagnetic” region $\gamma \in [0, 1]$ and the “antiferromagnetic” region $\gamma \in (1, \infty]$.
- For $z = 4$, when $\gamma_z = 0$, we will observe critical behavior in the basal plane only at the dual point $\gamma \rightarrow \infty$.
- For $4 < z < 7$, we have an transition to order in the basal plane in the z -antiferromagnetic region; in both such cases $\gamma_x < \gamma_{Az} \equiv \gamma_z^{-1}$, dividing this region into
 - a fully disordered regime $1 < \gamma < \gamma_x$,

⁵ Until now we have called γ_z γ_c instead.

⁶ Due to how γ appears in the deformation, any phase information it contains can be erased by a local unitary transformation; alternatively, we may say that the formulas we have used γ in should more properly have had $|\gamma|$.

- a z -disordered/ xy -ordered regime $\gamma_x < \gamma < \gamma_{Az}$, and
- a fully ordered regime $\gamma > \gamma_{Az}$,

whereas the basal plane is disordered throughout the “ferromagnetic” region $\gamma < 1$.

- For $z = 7$, the transition into will occur at the “decoupling” point $\gamma = 1$; thus the basal plane will be disordered throughout the “ferromagnetic” region and will obtain ferromagnetic order throughout the “antiferromagnetic” region.
- For $7 < z < 10$, we will have $\gamma_z < \gamma_x < 1$, such that, within the antiferromagnetic region, there is
 - an easy-axis regime (with z order and no x order) $\gamma \in [0, \gamma_z)$,
 - a fully-disordered regime $\gamma \in (\gamma_z, \gamma_x)$,
 - and an easy-plane regime (with x order and no z order) $\gamma \in (\gamma_x, 1)$.
- For $z = 10$, when $\gamma_x = \gamma_z = 1/2$, there is only symmetry-axis order when $\gamma > 1/2$ and only basal-plane order when $1/2 < \gamma < 1$.
- For $z > 10$, $\gamma_x < \gamma_z$ and so there will be
 - a phase where the symmetry axis spontaneously orders and the basal plane does not, with $\gamma \in [0, \gamma_x)$,
 - a phase with spontaneous symmetry breaking in both the symmetry axis and the basal plane for $\gamma \in (\gamma_x, \gamma_z)$ (it is easy to reason that we will have an easy axis for $\gamma < 1/2$ and an easy plane for $\gamma > 1/2$; we will indeed see that this is the case), and
 - a phase where the basal plane spontaneously orders and the symmetry axis does not, for $\gamma \in (\gamma_z, 1)$.

We explore these phase diagrams for $z \in [8, 12]$ in Fig. 9.

In the latter case, where $z > 10$ and spontaneous symmetry breaking occurs in both the symmetry axis and the basal plane for the region (γ_x, γ_z) , it is worth exploring the behavior of the system some more. As noted in subsection III, we can define an infinite ground state whenever a fixed point for our recursion relations exist; in particular, there will be a family of $+z$ -polarized ground states for $\gamma < \gamma_z$ and a family of e.g. $+x$ -polarized ground states for $\gamma > \gamma_x$. In Fig. 9 we see evidence that in the “hard-plane” case $\gamma \in (\gamma_x, 1/2)$, $+x$ polarization is unstable, and numerical error

compounded by a recursive method creates polarization along the symmetry axis. Meanwhile, in the stable “easy-axis” and “easy-plane” cases ($+z$ polarization for $\gamma \in (0, 1/2)$ and $+x$ polarization for $\gamma \in (1/2, 1)$), we have a family of ground states for a Hamiltonian that is known to have a phase transition within the region in question. However, we are unable to find any evidence that the one state “sees” the transition in the other direction, i.e. any nonanalyticities in the $+z$ -polarized state at γ_x or in the $+x$ -polarized state at γ_z .

VI. DISCUSSION

We have analyzed AKLT systems on the Bethe lattice with an arbitrary number of decorations on each edge. Our results – for example, that AKLT systems on singly-decorated Bethe lattice do not exhibit order for $z \leq 10$ – complement previous works which have shown that it is easier to establish and lower-bound the gap of such systems [10–13] in that our results imply that these systems are significantly further from order or criticality than the corresponding systems on the “bare” lattice.

Based on our analysis, we have then developed AKLT-based models with behavior exactly determined by recurrence relations. In one of these systems, in which we used frustration to tune the strength of interactions between sites without breaking $SU(2)$ symmetry, we found a continuous phase transition for the $z > 4$ cases in which the AKLT state on the undecorated Bethe lattice is antiferromagnetically ordered, and exactly determined critical exponents $\xi \sim \Delta\gamma^{-1}$, $m \sim \Delta\gamma^{-1/2}$, and $S \sim r^{-1/2}$ for S a combination of observables designed to observe boundary effects at a radius r . This suggests that similar decorations may be used to perturb more physical ordered frustration-free systems, such as the AKLT state on the cubic lattice[14], to phase transitions.

In another, in which we began with a singly-decorated Bethe lattice and then deformed the decoration to obtain phase transitions, we saw competing order in the symmetry axis and the basal plane, including coexisting ground states with each order. It is notable, if not surprising given the definition of frustration-freeness, that these states are all simultaneously true ground states, with the same energy. We may ask if this is more generally the case for frustration-free systems: if, when a (frustration-freeness-preserving) deformation explicitly adds anisotropy in this way to a system that already exhibits spontaneously-broken symmetry, it is generally possible to define states in the thermodynamic limit that order along both “easy” and “hard” axes – and, if so, whether there is a continuous phase transition that is effectively undetectable by manipulations of a stable ground state.

ACKNOWLEDGEMENTS

I would like to thank Tzu-Chieh Wei for suggesting the topic and for fruitful discussions while the ideas in this work were being developed. This work was supported by the National Science Foundation under Grant No. PHY 1915165.

-
- [1] I. Affleck, T. Kennedy, E. H. Lieb, and H. Tasaki, Rigorous results on valence-bond ground states in antiferromagnets, *Phys. Rev. Lett.* **59**, 799 (1987).
 - [2] I. Affleck, T. Kennedy, E. H. Lieb, and H. Tasaki, Valence bond ground states in isotropic quantum antiferromagnets, *Communications in Mathematical Physics* **115**, 477 (1988).
 - [3] M. Fannes, B. Nachtergaele, and R. F. Werner, Ground states of vbs models on cayley trees, *Journal of statistical physics* **66**, 939 (1992).
 - [4] R. Werner, Construction and study of exact ground states for a class of quantum antiferromagnets, *Revista Brasileira de Física* **19** (1989).
 - [5] B. Nachtergaele, Working with quantum markov states and their classical analogues, in *Quantum probability and applications V* (Springer, 1990) pp. 267–285.
 - [6] F. Fidaleo and F. Mukhamedov, On factors associated with quantum markov states corresponding to nearest neighbor models on a cayley tree, in *Quantum Probability And Infinite Dimensional Analysis* (World Scientific, 2005) pp. 237–251.
 - [7] L. Accardi, F. Mukhamedov, and A. Souissi, On construction of quantum markov chains on cayley trees, in *Journal of Physics: Conference Series*, Vol. 697 (IOP Publishing, 2016) p. 012018.
 - [8] B. Friedman, A density matrix renormalization group approach to interacting quantum systems on cayley trees, *Journal of Physics: Condensed Matter* **9**, 9021 (1997).
 - [9] D. Nagaj, E. Farhi, J. Goldstone, P. Shor, and I. Sylvester, Quantum transverse-field Ising model on an infinite tree from matrix product states, *Phys. Rev. B* **77**, 214431 (2008), arXiv:0712.1806 [cond-mat.stat-mech].
 - [10] H. Abdul-Rahman, M. Lemm, A. Lucia, B. Nachtergaele, and A. Young, A class of two-dimensional AKLT models with a gap, in *Contemporary Mathematics*, Vol. 741, edited by H. Abdul-Rahman, R. Sims, and A. Young (American Mathematical Society, Providence, 2020) pp. 1–21.
 - [11] N. Pomata and T.-C. Wei, AKLT models on decorated square lattices are gapped, *Phys. Rev. B* **100**, 094429 (2019).
 - [12] W. Guo, N. Pomata, and T.-C. Wei, The AKLT models on the singly decorated diamond lattice and two degree-4 planar lattices are gapped (2020), arXiv:2010.03137 [cond-mat.str-el].
 - [13] N. Pomata and T.-C. Wei, Demonstrating the Affleck-Kennedy-Lieb-Tasaki spectral gap on 2D degree-3 lattices, *Phys. Rev. Lett.* **124**, 177203 (2020).

- [14] S. A. Parameswaran, S. L. Sondhi, and D. P. Arovas, Order and disorder in AKLT antiferromagnets in three dimensions, *Phys. Rev. B* **79**, 024408 (2009).